Current Biology *18*, 900–905, June 24, 2008 ©2008 Elsevier Ltd All rights reserved DOI 10.1016/j.cub.2008.05.013

Report

Mutagenic Capacity of Endogenous G4 DNA Underlies Genome Instability in FANCJ-Defective *C. elegans*

Evelien Kruisselbrink,[1,2] Victor Guryev,[1,2] Karin Brouwer,[1] Daphne B. Pontier,[1] Edwin Cuppen,[1] and Marcel Tijsterman[1,*]

[1]Hubrecht Institute
Royal Netherlands Academy of Arts and Sciences & University Medical Centre Utrecht
Uppsalalaan 8
3584 CT, Utrecht
The Netherlands

Summary

To safeguard genetic integrity, cells have evolved an accurate but not failsafe mechanism of DNA replication. Not all DNA sequences tolerate DNA replication equally well [1]. Also, genomic regions that impose structural barriers to the DNA replication fork are a potential source of genetic instability [2, 3]. Here, we demonstrate that G4 DNA—a sequence motif that folds into quadruplex structures in vitro [4, 5]—is highly mutagenic in vivo and is removed from genomes that lack *dog-1*, the *C. elegans* ortholog of mammalian FANCJ [6, 7], which is mutated in Fanconi anemia patients [8–11]. We show that sequences that match the G4 DNA signature $G_{3-5}N_{1-3}G_{3-5}N_{1-3}G_{3-5}N_{1-3}G_{3-5}$ are deleted in germ and somatic tissues of *dog-1* animals. Unbiased aCGH analyses of *dog-1* genomes that were allowed to accumulate mutations in >100 replication cycles indicate that deletions are found exclusively at G4 DNA; deletion frequencies can reach 4% per site per animal generation. We found that deletion sizes fall short of Okazaki fragment lengths [12], and no significant microhomology was observed at deletion junctions. The existence of 376,000 potentially mutagenic G4 DNA sites in the human genome could have major implications for the etiology of hereditary FancJ and nonhereditary cancers.

Results and Discussion

Previously, we have built transgenic *C. elegans* strains to monitor frame-shifting errors that occur at DNA repeats [13] and observed that monoC/G tracts were much more error prone than monoA/T tracts of identical lengths. Although this observation is in agreement with worm and yeast data on endogenous repeats [14, 15], we reasoned that genome rearrangements other than microsatellite instability could also contribute. This notion was fueled by the identification of *dog-1*, a DNA helicase that protects monoC/G but not monoA/T tracts from being deleted [6]. Crossing a deletion allele of *dog-1* into reporter lines that monitor frame-shifting at mono(C/G)23 tracts, however, failed to result in significantly increased reporter expression, likely because the tract is a very strong inducer of DNA frame-shifts, resulting in many ORF-restoring events per animal even in a mismatch repair-proficient background.

To specifically investigate deletion induction at monoC/G tracts, we developed a phenotypic assay making use of the nonsymmetrical way deletions are induced at such sequences in *dog-1*-deficient animals: deletions were previously found to start immediately 5′ of a monoC/G tract to end at seemingly random locations a few hundred nucleotides downstream [6]. We therefore placed a monoC tract followed by mutiple stop codons downstream of a reporter gene's start codon, but in a nonessential region (Figure 1A). Only deletions that take out the mononucleotide repeat and all stop codons can bring the LacZ start codon in-frame with the downstream ORF. For clarity, we will adopt the term monoG- or G tract-induced deletions for these types of DNA rearrangements. Figure 1B shows lacZ-expressing cells that appear in ~0.3% of *dog-1*-defective animals, but these are never observed in wild-type ($n > 10^6$). The observed patterns of expression were typical for stochastic events happening during DNA replication in animal development: both early and late events were observed, as reflected by many or few cells that express B-galactosidase (Figure 1B). All somatic tissues were susceptible. Note also that a single reversion event leads to expression in all progeny cells, which in combination with the nematode's invariant cell lineage allows us to trace back genomic deletions to a single somatic event during embryogenesis. Molecular PCR-based analysis of individual worms showed that these transgenes faithfully recapitulate the previously observed mutation spectrum at endogenous monoG tracts [15]: only in *dog-1*, but not in wild-type animals, we observed deletions that take away almost the entire G tract together with 5′ flanking sequence (Figure 1C and see Figure S1A available online). MonoA tracts are not susceptible to *dog-1*-dependent deletion formation (Figure S1B).

We next questioned, what makes monoG tracts unstable? Is it because they are extremely prone to replication slippage (monoG > monoA), and could deletions be the result of error-prone repair of DNA intermediates created by DNA mismatch repair proteins? We tested whether monoG tract instability was dependent on functional mismatch repair, but we found no effect of genetically inactivating *msh-6* on deletion induction in a *dog-1*-proficient or -deficient background (Figure S1). Rose and colleagues recently published a survey of *C. elegans* strains with mutations in various types of DNA repair pathways, all of which had wild-type behavior for their ability to maintain monoG tracts in their genomes [7, 16]. In agreement, we found that none of the major genome-maintenance pathways were involved in preventing monoG tract instability, by using our sensitive transgenic assay or population-based PCR techniques (Figures S1C–S1F; we estimate that we would be able to detect a deletion frequency that is <1% of the deletion frequency observed in *dog-1* mutant animals). These also included Werner's and Bloom's Syndrome helicases—these proteins have been shown in vitro to unwind secondary structures that are formed in G-rich ssDNA [17, 18].

In an unbiased approach to identify genetic determinants, we mutagenized transgenic animals that carry monoG tract instability reporters and assayed progeny animals that express

*Correspondence: tijsterman@niob.knaw.nl
[2]These authors contributed equally to this work

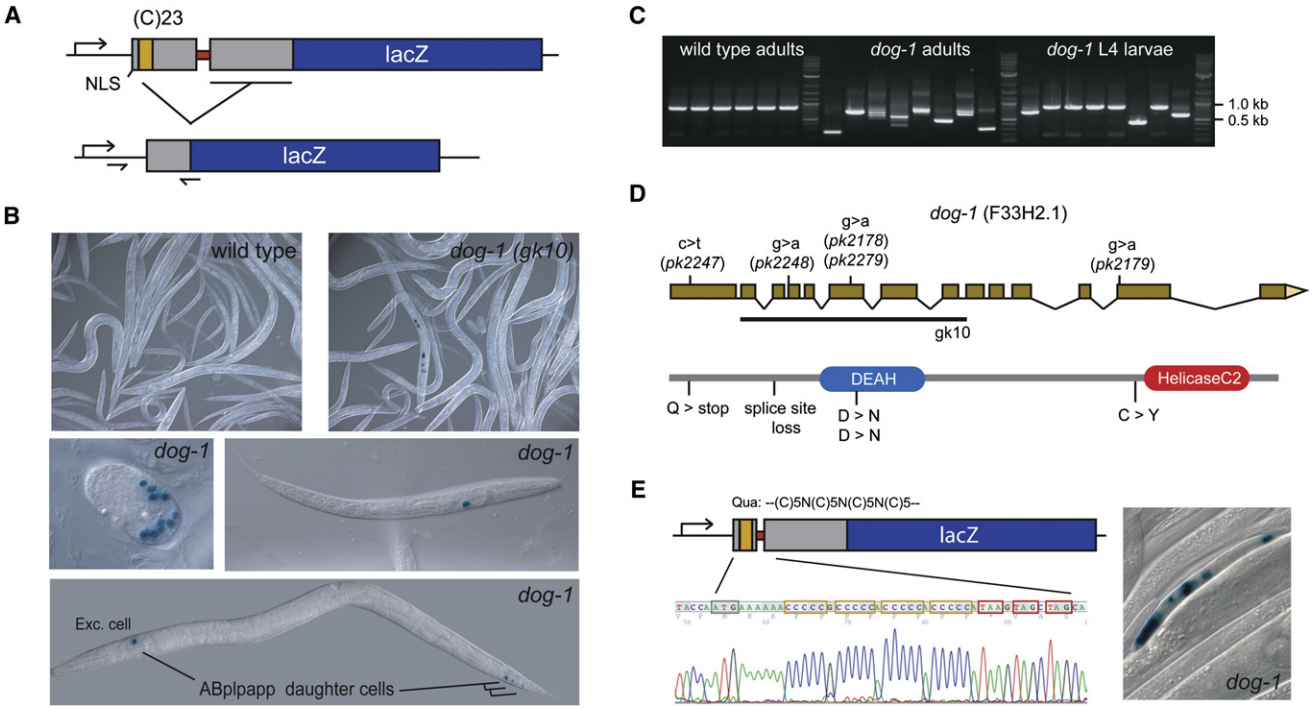

Figure 1. A Transgenic Reporter Assay to Monitor G Tract-Induced Genomic Rearrangements

(A) Schematic drawing of a reporter LacZ gene that is made dysfunctional by interrupting the LacZ ORF with a $(C)_{23}$ repeat in the nontemplate strand (yellow) and an in-frame ORF (gray) that contains stop codons (red). Only mutagenic events that delete the C-stretch (G tract) together with 3′ flanking sequences can bring LacZ in-frame with the upstream start codon resulting in detectable B-galactosidase expression.

(B) *dog-1*-deficient transgenic animals express B-galactosidase as a result of stochastic DNA rearrangements in somatic cells during development. The upper right panel depicts expression in a subset of intestinal cells. Unspecified early and late events are depicted in the middle panels. The bottom panel shows expression in cells located at the posterior and anterior ends of the *C. elegans* bodyplan as a result of a genomic rearrangement in the joint founder cell ABplpapp.

(C) Molecular analysis of G tract-induced deletion formation in single wild-type or *dog-1*-deficient adults or larvae of the L4 stage by PCR amplification of sequences flanking transgenic G tracts (primers indicated in [A]).

(D) Schematic illustration of independently derived *dog-1* alleles that were identified in a clonal F2 forward mutagenesis screen, as well as the *gk10* reference allele. The motif structure of the encoded protein is depicted underneath, as well as how the mutations affect the protein's structure or function.

(E) Schematic and sequence representation of a functional reporter system that colorimetrically visualizes G4 DNA fragility. Here, the LacZ reporter contains early stop codons immediately downstream of a $C_5NC_5NC_5NC_5$ sequence that predicts a G4 DNA quadruplex structure in the template strand. B-galactosidase-expressing cells identify G4 DNA-induced genomic deletion events.

B-galactosidase in sublineages, indicative of monoG tract-induced rearrangements. We identified 5 mutants in ~4800 genomes, all of which were loss-of-function mutations in *dog-1* (Figure 1D). Although the forward and reverse genetic approaches presented here have not reached saturation levels, they fuel the hypothesis that monoG tracts may represent a special type of premutagenic lesion that is not acted upon by any of the known major DNA-repair pathways.

What features of monoG tracts make these sequences uniquely depend on functional DOG-1? To address this question, we took a genomics approach to identify additional fragile sites and look for common denominators. DNA of clonally grown *dog-1* cultures, to establish so-called "mutation accumulation" (MA) lines (Figure 2A), was assayed by comparative genome hybridization (CGH). We built custom-made *C. elegans* arrays, onto which we spotted a tiling path of ~300,000 overlapping probes covering the complete left arm of chromosome V, as well as ~81,000 probes aimed to investigate sequences surrounding candidate fragile loci: (1) nucleotide repeats of various types, (2) palindrome-resembling sequences potentially able to form hairpins in ssDNA, (3) G4 DNA sequences matching the signature $G_{3-5}N_{1-7}G_{3-5}N_{1-7}G_{3-5}N_{1-7}G_{3-5}$ (ssDNA containing such motifs have in vitro been shown to fold into four-stranded secondary structures, called quadruplexes [19, 20]), and (4) G-rich telomeric DNA. Figure 2B displays a log-plot of the entire left arm of LGV for one *dog-1* MA strain compared to wild-type Bristol N2; Figure 2C exemplifies two typical deletion profiles that were found at candidate fragile loci. In total, we identified 69 germline deletions in 16 *dog-1* MA lines, versus zero in N2, and we sequenced 51 of those (see Table S1 for a complete list plus characteristics), which allows us to draw conclusions with respect to frequency, distribution, size, sequence requirements, and flanking sequences. We will focus on three key findings.

Most importantly, we found that G4 DNA sites, but only G4 DNA sites, are fragile in *dog-1*-deficient genomes. The chromosome V tiling path, covering 7% of the entire genome, identified eight deletions, all of which map to monoG tracts. In support of such a narrow spectrum of fragile sequences, we found no DNA rearrangements at telomeric sites at 93 A_{17-24}, at 599 $(A/G)_{17-24}$, and at ~1000 sequences that could potentially form DNA hairpins. In contrast, the candidate approach revealed 62 deletions at large monoG tracts ($G_{n>14}$), 4 deletions at monoG-like sequences (having 1 or 2 nucleotides that interrupt a monoG tract), and 3 deletions at sequences

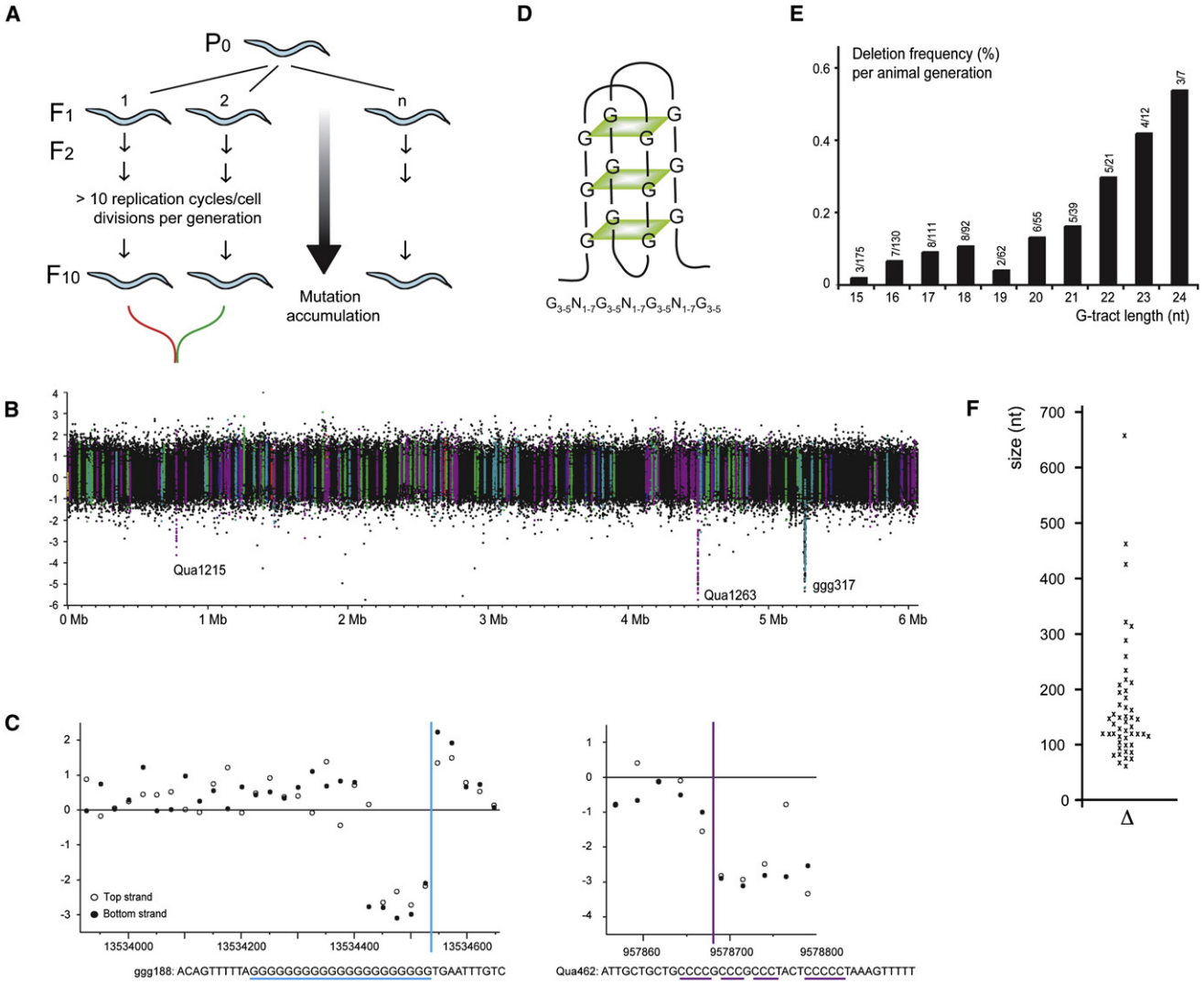

Figure 2. Array Comparative Genomic Hybridization Identifies G4 DNA Fragile Sites

(A) Culturing scheme leading to *dog-1* mutation accumulation (MA) lines. Here, we took advantage of the fact that *C. elegans* can be maintained as self-fertilizing hermaphrodites: we singled out the progeny of one parental animal (P0), allowed these sublines to grow for 10 generations, and then picked one (F10) animal to establish a new culture of which the DNA represents the genome of that F10 animal. These MA lines have thus independently gone through >100 rounds of DNA replication.

(B) A typical log plot of ~300,000 tiled DNA probes covering the left arm of chromosome 5 is displayed for MA-14 over wild-type (N2). Probes that flank (<1000 bp) candidate fragile sites are color coded: monoA tracts in red, monoG in blue, non-monoG G4 DNA in purple, palindromic sequences in green, and subtelomeric sequences in yellow. This strain suffered three deletions in this interval, which are indicated.

(C) Graphical illustrations of a 144 bp deletion at ggg188 in MA-20 and a 157 bp deletion at Qua462 in MA-13. Closed and open circles represent probes against the chromosomal top and bottom strand. The x axis indicates the chromosomal position on the *C. elegans* physical map; colored lines indicate the positions of the G4 DNA sequences of which the sequence is given underneath the log plots.

(D) Schematic representation of antiparallel quadruplex DNA in which planar rings of four guanines (G-quartets) can stack on top of each other, thereby forming an unusual DNA structure that is thermodynamically stable under physiological conditions.

(E) Graphical representation of deletion frequencies as a function of G tract length. The absolute number of G(n)-induced deletions (for given n) are divided by the number of G(n)'s in the *C. elegans* genome. These numbers are plotted above the bars. Note that we used only deletions induced by monoG tracts that are not part of larger G4 DNA sequences: $(G)_{15\text{-}24}N_{1\text{-}7}(G)_{>2}$ and $(G)_{>2}N_{1\text{-}7}(G)_{15\text{-}24}$ were excluded.

(F) Size distribution of G4 DNA-induced germline deletions (n = 49).

that deviate from the monoG type (e.g., GGGGGagtaGGGc GGGcGGGG) but have the potential to fold into a quadruplex structure: having four stretches of at least three guanines interrupted by nucleotides of any type (Table S1; Figures 2C and 2D). In all deletions, the fragile site is taken out almost completely together with 5′ (but not 3′) flanking DNA. We argue that the unique feature that makes monoG tracts unstable is that they match the G4 signature and thus have the ability to adopt a quadruplex structure. Although the relative abundance of deletions at monoG tracts versus non-monoG G4 DNA (62 versus 3) seems to contradict the relative abundance of the two classes of DNA sequence in the *C. elegans* genome (525 versus 1742), this can be fully explained by assuming that longer monoG sequences have a greater degree of liberty to fold into a quadruplex. For example, non-monoG Qua462 (Figure 2C) can fold into 6 different quadruplex structures, while

a monoG sequence of similar size (22 nt) offers 362 possibilities. In support of this notion, we observed that the deletion-inducing capacity of G4 DNA increased with tract length and G-ratio (Figure 2E; data not shown).

Another notable observation from the aCGH data is the total lack of sequence similarity around the deletion junctions. We found no evidence for microhomology-driven repair (or bypass) by scanning 51 germline deletions at different genomic loci or 18 deletions at one transgenic G4 DNA sequence in somatic cells (Table S1 and Figure S1A). In particular, the lack of apparent homology between nucleotides positioned upstream but within the deleted segment with unaffected sequences immediately downstream of the fragile site argues against mechanisms involving microhomology-dependent DSB repair at G4 DNA-blocked replication forks.

Finally, we observed that deletions are predominantly of small size. The array design combined with the algorithms we developed allow us to detect deletions larger than ~50–70 base pairs, but there is no upper constraint, apart from in vivo limitations where large deletions may cause lethality. Indeed, we identified deletions in the range of 63–7347 nucleotides. However, in 88% of the cases, less than 300 bp have been deleted, the average size of which is 141 bp. Such size distribution hints at a model in which the deletion size is determined by the distance between a lagging strand replication fork that is stalled at a G4 DNA sequence to the nearest upstream Okazaki fragment (the average length of eukaryotic Okazaki fragments being ~300 bp [12]).

We estimate that our CGH data is derived from ~1600 replicated genomes. Although most deleted sites were represented only once, we found two exceptions: ggg317 (3×) and ggg463 (2×). This indicates that the mutagenic potential of these sequences can be enormous: ~4% for ggg317 per animal generation. The majority of G4 DNA sites, however, have not been deleted, likely because the rate of deletion induction per site is far below the rate required to see it here. Alternatively, many sites are not intrinsically mutagenic; previous work suggested that only half of the monoG tracts are fragile, leading to the speculation that monoG tract fragility could predict whether DNA sequences are replicated via the leading or lagging strand [6]. We here show that this is not the case: all tested monoG $_{>20}$ tracts are mutagenic (Figures 3A and 3D). In addition, we identified two DNA tracts that were only 39 bp apart but located in opposite DNA strands, and both are fragile (Figure 3B). Although we concur with the idea that quadruplexes are preferentially formed in the lagging strand, our observation is consistent with data from other systems suggesting that there are no fixed origins of replication during development [21].

Next, we addressed the question of whether all sequences that match the used G4 DNA signature are fragile. First, we tested a custom-made G4 DNA sequence $G_5NG_5NG_5NG_5$ in transgenic reporter animals and found it to induce deletions in a *dog-1*-dependent manner (Figure 1E). Second, we developed more sensitive PCR assays on endogenous loci—we titrated PCR conditions to optimally amplify smaller than wild-type products—and found that all sequences that match the G4 DNA signature but have a limited number of nucleotides in between the G4 DNA legs are fragile (Figures 3C and 3D). In contrast, G3 DNA sites (sequences that resemble G4 but miss one "leg" of a possible quadruplex) were never fragile. We also investigated one case in which a monoG tract had a $(G)_3$ tract 4 nt away at its 3′ flank. We found that six out of seven deletions started close to the $(G)_3$ sequence (Figure 3E), >7 nucleotides away from the monoG tract, indicating that the start of the fragile site was determined by the extra $(G)_3$ leg and not by the monoG tract.

Our molecular analyses demonstrate that endogenous sequences that have the ability to fold into quadruplex structures depend on DOG-1 to persist in *C. elegans* genomes. How do cells deal with these replication-blocking sequences? One previously suggested explanation [6] involves the unwinding of the quadruplex structure by DOG-1/FancJ's helicase activity to allow replication to proceed. Such a scenario would, however, not explain why *dog-1* animals are also sensitive to DNA crosslinks ([7]; Figure S2), because these cannot be unwound. This could point to a dual function of DOG-1: operating together with other Fanc proteins in crosslink repair but acting independently of them in a genome-maintenance pathway that prevents loss of G4 DNA. Alternatively, quadruplexed DNA constitutes strong replication impediments also in the presence of DOG-1, and replicative bypass is established not via unwinding of the quadruplex but via invasion and subsequent replication of the nearby already-replicated leading strand. The helicase activity of DOG-1 could help to unwind the replicated leading strands dsDNA to allow DNA synthesis. Such activity could also be envisaged for repair of crosslink damage [22].

The question of which enzymatic activities are involved in converting the premutagenic lesion (the quadruplex) to loss of sequence information (a deletion) is unanswered. Rose and colleagues have identified factors (e.g., homologous recombination proteins) whose loss stimulated deletion induction at monoG tracts in *dog-1* animals [16], suggesting that these factors play a role in an error-free way of dealing with G4 DNA. Loss of G4 DNA is, however, a consequence of an error-prone pathway. Candidate gene approaches have thus far suggested that none of the repair pathways that operate on DNA double-strand breaks (DSBs) are involved: inactivation of components of nonhomologous end joining (NHEJ), HR, or single-strand annealing (SSA) did not suppress deletion formation in a *dog-1* background ([16]; Figure S1). The notion that NHEJ components are not required is all the more surprising in the light of the observed lack of obvious homology at the deletion junctions.

Our transgenic setup, which perfectly mimics endogenous G4 DNA fragility, now allows a further investigation of the genetic and molecular determinants that influence replication progression in vivo at known locations that are amenable to genetic manipulation.

In summary, we have provided evidence that G4 DNA sequences that have the potential to fold into replication blocking quadruplex structures are intrinsically mutagenic in live animals. To prevent massive genome rearrangements at G4 DNA sites, cells require a specialized genome-protection mechanism that involves *C. elegans* FancJ, but not any of the other genes causally linked to Fanconi anemia [7, 23, 24]. Future work will have to uncover whether these fragile sites—there are more than 376,000 predicted G4 sites in the human genome [25]—are causally linked to at least part of the genomic rearrangements seen in tumors of human FancJ patients or in nonhereditary cancers.

Experimental Procedures

Strains and Culturing Conditions

See Supplemental Data for the *C. elegans* strains that were used in this study. Animals were grown at 20°C [26]. Transgenic strains were created via biolistic transformation or via gonadal injections followed by integration

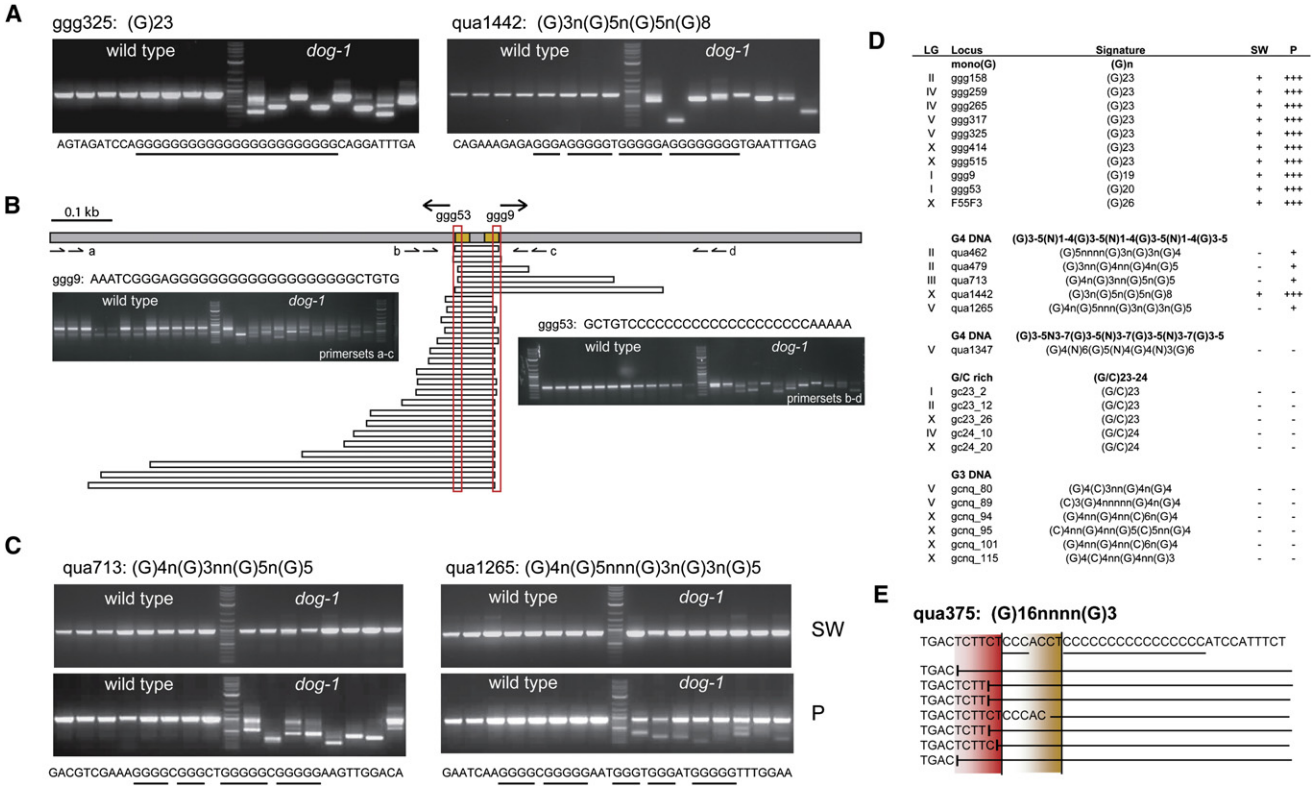

Figure 3. Mutagenic Determinants of Endogenous G4 DNA Sequences

(A) PCR analysis of endogenous G4 DNA sequences ggg325 and qua1442 on single wild-type and *dog-1(pk2247)* gravid animals (n = 8), separated by a DNA size marker containing lane. Both wild-type products are ~0.9 kb.

(B) Schematic diagram of an endogenous locus that contains two G4 DNA tracts having opposite polarity. The sequences are given above gel images that display PCR analysis on these loci in wild-type and *dog-1* mutant animals (n = 12). For each genetic background, five gravid animals were pooled in one sample. A representative set of smaller than wild-type bands, obtained with primers a and d, were purified and sequenced. The resulting deletions are graphically displayed beneath the locus diagram. The red boxing is to highlight that all deletions are on one site flanked by G4 DNA flanking sequence; that border defines the fragile G4 sequence.

(C) Single worm (SW)- and population (P)-based (10^4–10^5 animals) PCR analysis of G4 DNA sequences qua713 and qua1265 for the indicated genotype (n = 8). Wild-type products are ~1 kb.

(D) Schematic sum up of endogenous G4 DNA instability in *dog-1(pk2247)* ranked per type and chromosome number (LG). A + marking indicates a deletion frequency of >6% (2 smaller bands in 32 samples); +++ means that individual bands were difficult to discriminate (instead, DNA smears are observed resulting from amplification of many differently sized [deletion-containing] fragments per DNA sample).

(E) A graphic illustration of the deletion start sites that occur at G4 DNA sequence qua375. Sequences that are not deleted are depicted. For qua375, there are two potential deletion initiation sites: deletions in the red zone likely result from a DNA replication-blocking quadruplex that includes the 3′ $(G)_3$ sequence (or 5′ $(C)_3$), whereas a quadruplex made up of only the upstream (G)16 sequence is predicted to trigger deletion induction in the yellow zone.

of extrachromosomal arrays by X-ray irradiation. B-galactosidase expression was assayed as described previously [13].

Array Design and Bio-informatical Analyses

We used WS140 *C. elegans* genome built to design 40- to 60-mer probes with fixed 72°C Tm for Nimblegen 388.5k microarray chips according to manufacturer's instructions. On average, adjacent probes overlap 50%. The array (precise design available upon request) contained a 7.7 Mb tiling path of LGV as well as probes directed at sequences that flank candidate fragile sites: all candidate fragile sites were flanked on each site with 10 probes (top and bottom strand) except monoG tracts; these were flanked by 60 upstream and 10 downstream probes. Nimblegen performed hybridizations for 20 DNA samples: 2 Bristol N2, 16 *dog-1* MA lines, and 2 DNA samples derived from the *dog-1* P0 animal. We predicted deletions by comparing hybridization intensity ratios of every MA line to N2. We created a deletion-candidate probe set that included probes with the most extreme ratios (0.1% from both tails of ratio distribution). Deletions were called if a sequence segment was represented by at least two of three consecutive probes in the candidate probe set. 96 DNA segments were chosen for PCR and sequence verification. aCGH data were confirmed by analyzing 96 genomic loci by PCR amplification and sequencing. Primers were designed to target strong candidate deletions—those were handpicked upon visual inspection of log plots of all regions that scored positive according to our algorithms—as well as a number of negative controls and cases that were ambiguous. This led to a 100% verification rate for the highest-scoring subset of candidate loci.

DNA Analysis and Reporter Cloning

Analysis of fragile sites on endogenous loci was performed with nested sets of primers (sequences available upon request), and PCR conditions were optimized per primer set to favor the amplification of smaller than wild-type bands. Reporter transgene cloning: for all variants, we started with pRP1821 [13] that contains a heat-shock driven GPF::lacZ ORF lacking a start codon; for pRP1878 (pkIs2165), we oligo-cloned an ATG-NLS-(C)23 sequence upstream of the GFP::lacZ ORF and then placed a stop codon at the XhoI site of GFP; for pRP3020 (lfIs17), we placed an ATG-(G4 DNA)-stop codon sequence in front of the GFP::LacZ fusion. pRP1889 contained a monoA tract at that position.

Supplemental Data

Two figures, one table, and Experimental Procedures are available at http://www.current-biology.com/cgi/content/full/18/12/900/DC1/.

Acknowledgements

We thank Ronald Plasterk for generous support; Marit Kosters and Astrid Eijkelenboom for technical assistance; the CGC, the knockout consortia, Simon Boulton, and Shohei Mitani for strains; and all Wormbase curators for building the platform that allows *C. elegans* genomic research. This work was supported by a ZonMW VIDI grant to M.T.

Received: March 21, 2008
Revised: April 17, 2008
Accepted: May 5, 2008
Published online: June 5, 2008

References

1. Harfe, B.D., and Jinks-Robertson, S. (2000). DNA mismatch repair and genetic instability. Annu. Rev. Genet. *34*, 359–399.
2. Brewer, B.J., Lockshon, D., and Fangman, W.L. (1992). The arrest of replication forks in the rDNA of yeast occurs independently of transcription. Cell *71*, 267–276.
3. Lambert, S., Watson, A., Sheedy, D.M., Martin, B., and Carr, A.M. (2005). Gross chromosomal rearrangements and elevated recombination at an inducible site-specific replication fork barrier. Cell *121*, 689–702.
4. Gellert, M., Lipsett, M.N., and Davies, D.R. (1962). Helix formation by guanylic acid. Proc. Natl. Acad. Sci. USA *48*, 2013–2018.
5. Sen, D., and Gilbert, W. (1988). Formation of parallel four-stranded complexes by guanine-rich motifs in DNA and its implications for meiosis. Nature *334*, 364–366.
6. Cheung, I., Schertzer, M., Rose, A., and Lansdorp, P.M. (2002). Disruption of dog-1 in *Caenorhabditis elegans* triggers deletions upstream of guanine-rich DNA. Nat. Genet. *31*, 405–409.
7. Youds, J.L., Barber, L.J., Ward, J.D., Collis, S.J., O'Neil, N.J., Boulton, S.J., and Rose, A.M. (2008). DOG-1 is the *Caenorhabditis elegans* BRIP1/FANCJ homologue and functions in interstrand cross-link repair. Mol. Cell. Biol. *28*, 1470–1479.
8. Levran, O., Attwool, C., Henry, R.T., Milton, K.L., Neveling, K., Rio, P., Batish, S.D., Kalb, R., Velleur, E., Barral, S., et al. (2005). The BRCA1-interacting helicase BRIP1 is deficient in Fanconi anemia. Nat. Genet. *37*, 931–933.
9. Levitus, M., Waisfisz, O., Godthelp, B.C., de Vries, Y., Hussain, S., Wiegant, W.W., Elghalbzouri-Maghrani, E., Steltenpool, J., Rooimans, M.A., Pals, G., et al. (2005). The DNA helicase BRIP1 is defective in Fanconi anemia complementation group J. Nat. Genet. *37*, 934–935.
10. Bridge, W.L., Vandenberg, C.J., Franklin, R.J., and Hiom, K. (2005). The BRIP1 helicase functions independently of BRCA1 in the Fanconi anemia pathway for DNA crosslink repair. Nat. Genet. *37*, 953–957.
11. Litman, R., Peng, M., Jin, Z., Zhang, F., Zhang, J., Powell, S., Andreassen, P.R., and Cantor, S.B. (2005). BACH1 is critical for homologous recombination and appears to be the Fanconi anemia gene product FANCJ. Cancer Cell *8*, 255–265.
12. Abdurashidova, G., Deganuto, M., Klima, R., Riva, S., Biamonti, G., Giacca, M., and Falaschi, A. (2000). Start sites of bidirectional DNA synthesis at the human lamin B2 origin. Science *287*, 2023–2026.
13. Tijsterman, M., Pothof, J., and Plasterk, R.H. (2002). Frequent germline mutations and somatic repeat instability in DNA mismatch-repair-deficient *Caenorhabditis elegans*. Genetics *161*, 651–660.
14. Denver, D.R., Feinberg, S., Estes, S., Thomas, W.K., and Lynch, M. (2005). Mutation rates, spectra and hotspots in mismatch repair-deficient *Caenorhabditis elegans*. Genetics *170*, 107–113.
15. Sia, E.A., Kokoska, R.J., Dominska, M., Greenwell, P., and Petes, T.D. (1997). Microsatellite instability in yeast: dependence on repeat unit size and DNA mismatch repair genes. Mol. Cell. Biol. *17*, 2851–2858.
16. Youds, J.L., O'Neil, N.J., and Rose, A.M. (2006). Homologous recombination is required for genome stability in the absence of DOG-1 in *Caenorhabditis elegans*. Genetics *173*, 697–708.
17. Fry, M., and Loeb, L.A. (1999). Human werner syndrome DNA helicase unwinds tetrahelical structures of the fragile X syndrome repeat sequence d(CGG)n. J. Biol. Chem. *274*, 12797–12802.
18. Sun, H., Karow, J.K., Hickson, I.D., and Maizels, N. (1998). The Bloom's syndrome helicase unwinds G4 DNA. J. Biol. Chem. *273*, 27587–27592.
19. Burge, S., Parkinson, G.N., Hazel, P., Todd, A.K., and Neidle, S. (2006). Quadruplex DNA: sequence, topology and structure. Nucleic Acids Res. *34*, 5402–5415.
20. Maizels, N. (2006). Dynamic roles for G4 DNA in the biology of eukaryotic cells. Nat. Struct. Mol. Biol. *13*, 1055–1059.
21. Gilbert, D.M. (2005). Origins go plastic. Mol. Cell *20*, 657–658.
22. Niedernhofer, L.J., Lalai, A.S., and Hoeijmakers, J.H. (2005). Fanconi anemia (cross)linked to DNA repair. Cell *123*, 1191–1198.
23. Mirchandani, K.D., and D'Andrea, A.D. (2006). The Fanconi anemia/BRCA pathway: a coordinator of cross-link repair. Exp. Cell Res. *312*, 2647–2653.
24. Levitus, M., Joenje, H., and de Winter, J.P. (2006). The Fanconi anemia pathway of genomic maintenance. Cell. Oncol. *28*, 3–29.
25. Huppert, J.L., and Balasubramanian, S. (2005). Prevalence of quadruplexes in the human genome. Nucleic Acids Res. *33*, 2908–2916.
26. Brenner, S. (1974). The genetics of *Caenorhabditis elegans*. Genetics *77*, 71–94.